THE JOURNAL OF BIOLOGICAL CHEMISTRY VOL. 291, NO. 26, pp. 13560–13570, June 24, 2016

Conversion of Fibroblasts to Parvalbumin Neurons by One Transcription Factor, Ascl1, and the Chemical Compound Forskolin*[S]

Received for publication, December 12, 2015, and in revised form, March 17, 2016 Published, JBC Papers in Press, May 2, 2016, DOI 10.1074/jbc.M115.709808

Zixiao Shi[‡§], Juan Zhang[‡§], Shuangquan Chen[‡§], Yanxin Li[‡§], Xuepei Lei[‡§], Huimin Qiao[‡§], Qianwen Zhu[¶], Baoyang Hu[‡], Qi Zhou[‡], and Jianwei Jiao[‡1]

From the [‡]State Key Laboratory of Stem Cells and Reproductive Biology, Institute of Zoology, Chinese Academy of Sciences, Beijing 100101, China, [§]University of Chinese Academy of Sciences, Beijing 100049, China, and [¶]Institute of Biophysics, Chinese Academy of Sciences, Beijing 100101, China

Abnormalities in parvalbumin (PV)-expressing interneurons cause neurodevelopmental disorders such as epilepsy, autism, and schizophrenia. Unlike other types of neurons that can be efficiently differentiated from pluripotent stem cells, PV neurons were minimally generated using a conventional differentiation strategy. In this study we developed an adenovirus-based transdifferentiation strategy that incorporates an additional chemical compound for the efficient generation of induced PV (iPV) neurons. The chemical compound forskolin combined with Ascl1 induced ~80% of mouse fibroblasts to iPV neurons. The iPV neurons generated by this procedure matured 5–7 days post infection and were characterized by electrophysiological properties and known neuronal markers, such as PV and GABA. Our studies, therefore, identified an efficient approach for generating PV neurons.

Parvalbumin interneurons are a small population of neurons that constitute the inhibitory modules of the cerebral cortex and hippocampus (1, 2). Although small in number and size, parvalbumin interneurons play important roles in a wide spectrum of brain functions, such as orchestrating the timing of various critical periods, synchronizing the electrical activities of certain brain cells, and rewiring the circuitry. The malfunction of these pivotal cells has been proven to be critical in autism, schizophrenia, and other neurodevelopmental disorders (1).

PV[2] neurons originate primarily from the medial ganglionic eminence of the subcortical telencephalon. They mature slowly and spread throughout the brain over time. Until now the procurement and generation of specific type of neurons has depended on direct differentiation from pluripotent stem cells, such as embryonic stem cells or induced pluripotent stem cells. This common approach has been used for the generation of PV neurons (3). The generation of PV neurons for research and therapeutic purposes by other approaches needs to be investigated.

Direct generation from one cell type to another provides a promising avenue for transplantable cells and holds great hope for cell-based therapy. Skin fibroblasts (mesodermal lineage) are an important source of starting cells that can be directly converted into a wide variety of cell types, including neurons (ectodermal lineage) (4, 5). Specific types of neurons, such as dopaminergic neurons (6–8), spinal motor neurons (9), and cholinergic neurons (10) have also been efficiently converted from mouse or human fibroblasts. Thus, for late-born and slowly maturing neurons such as parvalbumin interneurons, it might be possible to surpass the laborious process of differentiation by obtaining functional cells through the direct conversion from other types of cells.

Because of the side effect of integration associated with lentior retrovial delivery of exogenous genes, previous procedures used for transdifferentiation led to uncertainty in the genetic and epigenetic stability of the target cells. To explore suitable approaches for neuronal generation, we and other groups have developed a non-integrating transgene system for achieving induced neuronal cells from fibroblasts (11, 12). In such systems the desired cells can be directly obtained by the introduction of transcription factors, such as Ascl1, Brn2, and Ngn2. In addition, in the non-integrated transgene system, the addition of chemical compounds can efficiently promote the generation of functional neurons (13). Thus, we hypothesize that by combining the two effective approaches, the efficient generation of functional PV neurons from fibroblasts should be feasible.

To generate PV neurons through direct conversion, we set up a screening system based on the adenoviral expression of Ascl1 to screen candidate chemical compounds that could generate PV neurons. Finally, we found one chemical compound, forskolin, combined with one transcription factor Ascl1 efficiently converts fibroblasts to PV neurons.

Experimental Procedures

Animals—The young adult C57 mice were purchased from vital river company and kept in standard housing conditions. All of the animal studies were performed in accordance with

* This work was supported by the National Basic Research Program of China (2015CB964501 and 2014CB964903), the National Science Foundation of China (31371477), and the Strategic Priority Stem Cell Program (XDA01020301). The authors declare that they have no conflicts of interest with the contents of this article.

[S] This article contains supplemental Table 1.

Microarray data were deposited in NCBI Gene Expression Omnibus with the GEO accession number GSE79146.

[1] To whom correspondence should be addressed. E-mail: jwjiao@ioz.ac.cn.

[2] The abbreviations used are: PV, parvalbumin; iPV neuron, induced parvalbumin neuron; MEF, mouse embryonic fibroblast; TTX, tetrodotoxin; PSC, post-synaptic current; dpi, days post infection; AP, action potential; FSP1, fibroblast-specific protein 1; iN, induced neuron; CNQX, 6-cyano-7-nitroquinoxaline-2,3-dione; PTX, picrotoxin.

experimental protocols and approved by Animal Care and Use Committees at the Institute of Zoology, Chinese Academy of Sciences.

Fibroblast Isolation and Culture—We used E13.5 C57BL/6 or PV-GFP transgenic mouse embryos to isolate primary mouse embryonic fibroblasts. The head, vertebral column, dorsal root ganglia, and visceral organs were removed; the remaining tissues were dissected into small pieces and digested for 10 min in 0.25% trypsin (Invitrogen). The dissociated cells were cultured in high glucose DMEM (Invitrogen), supplemented with 10% fetal bovine serum (FBS) (Biochrom), 0.1 mM non-essential amino acids, and 2 mM Glutamax in a 37 °C and 5% CO_2 incubator. The cells became confluent in ~2–3 days and were passaged in a 1:4 split. MEFs were used between passages 2 and 4. Tail tip fibroblasts were obtained from the tail of 8-week-old mice.

Adenovirus Production and Infection—Ascl1 was cloned first in pEntr 3C vector (Invitrogen) and finally in pAD vector (Invitrogen) by homologous L/R recombination. The method of Ascl1 adenovirus packing followed the instruction of previous reports (11, 13). Then, we used the adenovirus to infect mouse embryonic fibroblasts or human embryonic fibroblasts twice for 4 h per day at multiplicities of infection (number of viral particles per cell) of 30 or 20. Twenty-four hours post infection, half of the culture medium was changed into neural medium (1 g/liter glucose DMEM/F-12/neural basal 2:2:1, 1×B-27, 10 or 20 ng/ml BDNF) every day for 2 successive days. Next, half of the medium was changed every 2 days until the cells were ready for immunostaining and electrophysiological experiments. 10 or 20 μmol/liter forskolin was freshly added in neural medium when culture medium was changed for 5 days.

Conversion Efficiency—We counted the conversion efficiency by using the neuronal purity as the percentage of Tuj1 cells relative to the total final population (11). We randomly selected 8–10 visual fields for each well and calculated the total cell number (at least 200 cells) visualized after DAPI staining and the total iN cell number indicated by Tuj1 staining. The efficiency was calculated by dividing the number of iN cells by the number of total cells in each visual field.

Immunofluorescence—iPV neurons were fixed with 4% paraformaldehyde in 0.1 mol/liter phosphate-buffered saline (PBS) for 20 min at room temperature and blocked with 5% BSA and 0.1% Triton X-100 in PBS for 30 min. Primary antibodies were diluted in antibody dilution solution (PBS with 1% BSA, 0.1% Triton X-100) in ratios from 1:100 to 1:1000, and secondary antibodies were diluted 1:1000 in antibody dilute solution. iPV neurons were incubated in primary antibodies overnight at 4 °C, and secondary antibodies were incubated for 60 min at room temperature.

The following primary antibodies were used: rabbit anti-fibronectin (1:100, BOSTER), rabbit anti-S100A4 (fibroblast-specific protein 1 (FSP1)) (1:100, Proteintech), mouse anti-GFAP (1:1000, Sigma), mouse anti-Nestin (1:200, Millipore), rabbit anti-Tuj1 (1:1000, Sigma), mouse anti-Tuj1 (1:1,000, Millipore), mouse anti-PV (1:400, Millipore), rabbit anti-GABA (1:4000, Sigma), rabbit anti-VGAT (1:500, Millipore), mouse anti-Map2a (1:500, Millipore), mouse anti-NeuN (1:300, Millipore), mouse anti-synapsin (1:500, Synaptic Systems), rabbit anti-vGLUT1 (1:1000, Synaptic Systems), mouse anti-GAD67 (1:1000, Millipore), rat anti-GFP (1:1000, MBL), rabbit anti-HB9 (1:100, Santa Cruz), and rabbit anti-TH (1:1000, Millipore), and DAPI (1:1000, Sigma). Alexa Fluor 488- and Alexa Fluor 546-conjugated secondary antibodies were obtained from Invitrogen. Cy2-, Cy3-, and Cy5-conjugated secondary antibodies were obtained from Jackson ImmunoResearch.

Real-time PCR Analysis—iPV neurons and wild-type neurons were cultured in neuron medium. MEFs were cultured in DMEM +10% FBS medium. All cells were washed with serum-free medium before collection. TRIzol extraction of total RNA was performed according to the manufacturer's instructions. 600 ng of total RNA was reverse-transcribed and then quantified using SYBR Green (Tiangen), and β-actin was used as the reference. Sequences of primers for real-time PCR were (F, forward; R, reverse): Map2a, AACCAATTCGCAGAGCAGGA (F) and GGGAGTTCCAGGGGTGATTG (R); NeuroD1, CAGCTCAACCCTCGGACTTT (F) and GGGGACTGGTAGGAGTAGGG (R); PV, GTCGATGACAGACGTGCTCA (F) and TTGTGGTCGAAGGAGTCTGC (R); KCNS3, TTCTATGCCACGTTGGCTGT (F) and AGACCGAAGCCCTACAGAGT (R); Cacn, AGGCTGCCCAATGGTTACT (F) and CTTAGCACCAGTCGTCCTCG (R); Kv1.1, TGCCCGGGTTATTGCCATTG (F) and TCCTTCAGCTCAGGGAGAGT (R); Kv1.2, TATCAGTCTGGGGGCAGGTT (F) and TGTAGCCTTCATCCTCCCGA (R); Kv1.6, vCACTCCGGACTTGAAGGCAA (F) and CCGCATAAGCTCGATGTGGA (R); Kv3.1, CCAGCGAACACACACACTTT (F) and ACCAGCATTCCAGACCACG (R); Kv3.2, AAGGCTCCCTATCAGACGCT (F) and GCAGTACTCTCCATGGGCTC (R); Nav1.1, GGCAACCTGACTCTGGTGTT (F) and TGGGAGTTTGCAGTCAGTGG (R); Nav1.2, CGCTCTCCTAGGTGCAATCC (F) and TCCTCTTCTTCCGTCGGTTC (R); exogenous Ascl1, TTAATACGACTCACTATAGGGA (F) and ATAGAGTTCAAGTCGTTGGAGTAGT (R); β-actin, GGCTGTATTCCCCTCCATCG (F) and CCAGTTGGTAACAATGCCATGT (R).

High Performance Liquid Chromatography (HPLC)—Liquid chromatography was performed by Agilent 1100 HPLC system (Agilent Technologies). The chromatographic separation was accomplished by Agilent Zorbax SB-C18 reserved phase column (280 × 6.4 mm, 5 μm) coupled with Agilent Zorbax Extend C18 guard column (10 × 6.4 mm, 5 μm). The column temperature was maintained at 25 °C. The mobile phase consisted of 40 mM Na_2HPO_4 in water (A) and an acetonitrile: methanol:water ratio of 45:45:10 (v/v/v) (B). Standard GABA and iPV neurons culture medium were diluted by ultrapure water. Samples were filtered by a 0.2-μm membrane before separation. The flow rate was 0.5 ml/min.

Enzyme-linked Immunosorbent Assay (ELISA)—Standard GABA and iPV neurons culture medium were used for coating overnight at 4 °C. The next day, PBS with 0.05% Tween 20 was used to wash wells for 4 times with slightly oscillation. Primary antibody (rabbit anti-GABA, 1:1000, Sigma) was added and incubated overnight at 4 °C. After washing, horseradish peroxidase-labeled secondary antibody was used for 1 h at 37 °C. Then, after washing, 0.1 ml of tetramethyl benzidine chromogenic solution (0.1 mg/ml, Solarbio) was reacted 5–10 min at

room temperature in a dark place and stopped by 0.1 ml of 1 M hydrochloric acid. Absorbance values were read by a microplate reader at 450 nm.

Transplantation of iPV Neurons in Vivo and Tissue Dissection—iPV neurons or MEFs were labeled with GFP by lentivirus infection and concentrated to $\sim 10^5$ cells/μl. 0.5 μl per site was transplanted into the brain hippocampal dentate gyrus area of 8–10-week-old epileptic C57BL/6 mice (anesthetized with 70 mg/kg pentobarbital sodium). 2–4 weeks post transplantation the mice were perfused with 0.9% saline and followed by 4% paraformaldehyde. The brains were removed and fixed in 4% paraformaldehyde overnight followed by gradient dehydration in 0.1 M PBS containing 5–30% sucrose for 2 days at 4 °C. Consecutive coronal sections (30 μm) were sliced using a Leica SM 2000R Sliding Microtome and stored in tissue collecting solution (25% glycerin, 25% ethylene glycol in 0.1 M PBS) at −20 °C until use. For migration studies, a single injection was made into the right dorsal CA3 region. For EEG and behavior experiments, transplantations were considered successful if the survival of GFP cells in the brain was evenly distributed in both hippocampus and cortex.

Electrophysiology; Cultured Cell Electrophysiological Detection—MEF-derived iPV cells were placed on glass coverslips for electrophysiological detection 7–14 days post infection. Whole cell patch clamp recordings in either voltage or current clamp mode were conducted to measure the voltage-activated sodium/potassium currents or action potentials, which were recorded using an Axopatch 200B or MultiClamp 700A amplifier (Molecular Devices). The electric signals were filtered at 2–10 kHz, digitized at 20–100 kHz (Digidata 1322A; Molecular Devices), and further analyzed using pClamp version 9.2 software (Molecular Devices). The intracellular solution contained 130 mM potassium gluconate, 20 mM KCl, 10 mM HEPES, 0.2 mM EGTA, 4 mM Mg_2ATP, 0.3 mM Na_2GTP, and 10 mM sodium phosphocreatine (at pH 7.3, 310 mOsM), and the pipette ranged from 2.0 to 4.0 megaohms. The extracellular fluid consisted of 124 mM NaCl, 3.3 mM KCl, 2.4 mM $MgSO_4$, 1.2 mM KH_2PO_4, 26 mM $NaHCO_3$, 2.5 mM $CaCl_2$, and 10 mM glucose (at pH 7.4, 310 mosM). Tetrodotoxin (TTX; 100 nM), AP5 (50 μM), CNQX (10 μM), PTX (50 μM), bicuculline (30 μM), or GABA (10 μM) were used in the bath solution for the detection of action potentials and spontaneous inhibitory postsynaptic currents.

Brain Slice Electrophysiological Detection—At 60–75 days after transplantation, mice were perfused with 0 °C artificial cerebrospinal fluid, and hippocampal coronal slices were prepared (300 μm in thickness). Slices were immerged in the incubation immediately at 32 °C for 10 min and perfused with 25 °C artificial cerebrospinal fluid with oxygen saturation. The cutting solution with sucrose contained 87 mM NaCl, 25 mM $NaHCO_3$, 25 mM glucose, 50 mM sucrose, 2.5 mM KCl, 1.2 mM NaH_2PO_4, 4 mM $MgCl_2$-$6H_2O$, and 0.5 mM $CaCl_2$. The external solution fluid (artificial cerebrospinal fluid) contained 118 mM NaCl, 25 mM $NaHCO_3$, 10 mM glucose, 2.5 mM KCl, 1.2 mM NaH_2PO_4, 1.3 mM $MgCl_2 \cdot 6H_2O$, and 2.5 mM $CaCl_2$ (at pH 7.3, 290 mOsM). Whole cell patch clamp recordings from GFP-labeled cells were performed at 40× using an upright, fixed-stage microscope (Olympus BX50WI) equipped with infrared differential interference contrast and epifluorescence optics. Patch pipettes (3–5 megaohms) were filled with an internal solution containing 140 mM potassium gluconate, 1 mM NaCl, 5 mM EGTA, 10 mM HEPES, 1 mM $MgCl_2$, 1 mM $CaCl_2$, 3 mM KOH, 2 mM ATP, and 0.2% biocytin (w/v), pH at 7.3, 300 mOsM. Recordings were obtained with an Axopatch 1D amplifier, filtered at 5 kHz, and recorded to pClamp 10.2 software (Clampfit, Axon Instruments). Spontaneous miniature postsynaptic currents (PSCs) were examined at a holding potential of −70 mV. Series resistance was typically <15 megaohms and was monitored throughout the recordings. Data were only used for analysis if the series resistance remained <20 megaohms and changed by ≤20% during the recordings. Recordings were not corrected for a liquid junction potential. Resting membrane potentials were measured immediately after breakthrough by temporarily removing the voltage clamp and monitoring voltage. For current-clamp recordings, electrophysiological properties were measured in response to a series of long (1000 ms) depolarizing current injections (50 pA steps, range = 100–1000 pA). Data analysis was performed using pClamp 10.2 (Clampfit, Axon Instruments), MiniAnalysis 6.0 (Synaptosoft), Microsoft Excel, and Sigmaplot 12.3 programs. A 2-min sample recording per cell was used for measuring miniature PSC characteristics. Events characterized by a typical fast rising phase and exponential decay phase were manually detected using the Mini Analysis program. The threshold for event detection was a current with an amplitude greater than three times the root mean square noise level.

Flow Cytometry Analysis—At 3, 7, and 14 days post infection, cells of infected MEFs were dissociated into single cell suspensions for flow cytometry screening, and GFP-positive cells were collected. The primary PV cells were sorted from P16 PV-GFP mouse brain, and induced PV cells were sorted from PV-GFP MEFs 14 days after infection. Living cells were analyzed by FACS Caliber apparatus (BD Biosciences) with FlowJo software (Tomy Digital Biology). The sorting cells were used to extract RNA and carried on further gene expression microarray analysis.

Gene Expression Microarray Analysis—Mouse genome-wide gene expression analysis was performed using GeneChip® Mouse Gene 2.0 ST Arrays (Affymetrix Inc.). Total RNA was extracted from MEFs, Ascl1+forskolin-treated iPV cells, FACS iPV cells, and FACS primary PV neurons from cortex of postnatal day 16 (P16) *PV*-GFP mouse; the total RNA was reverse-transcribed using an Amino AllylMessageAmp™ II aRNA Amplification kit (Ambion). For gene expression profiling analysis, mouse whole genome OneArray microarray v2 (MOA-002) chips were used with 41,345 mouse genome probes. Expression Console software (version 1.4.1, Affymetrix) was used to extract raw data and offer Robust Multi-array Average (RMA) normalization. Next, R software was employed to finish the basic analysis. Differentially expressed genes were then identified through -fold change. The threshold set for up- and down-regulated genes was a -fold change of ≥2.0. Afterward, GO analysis and KEGG analysis were applied to determine the roles of these differentially expressed mRNAs played in these GO terms or pathways. Microarray data were deposited in NCBI Gene Expression Omnibus with the GEO accession number GSE79146.

Statistical Analysis—Statistical analysis was evaluated by SPSS 16.0 software and assessed with normality and variance.

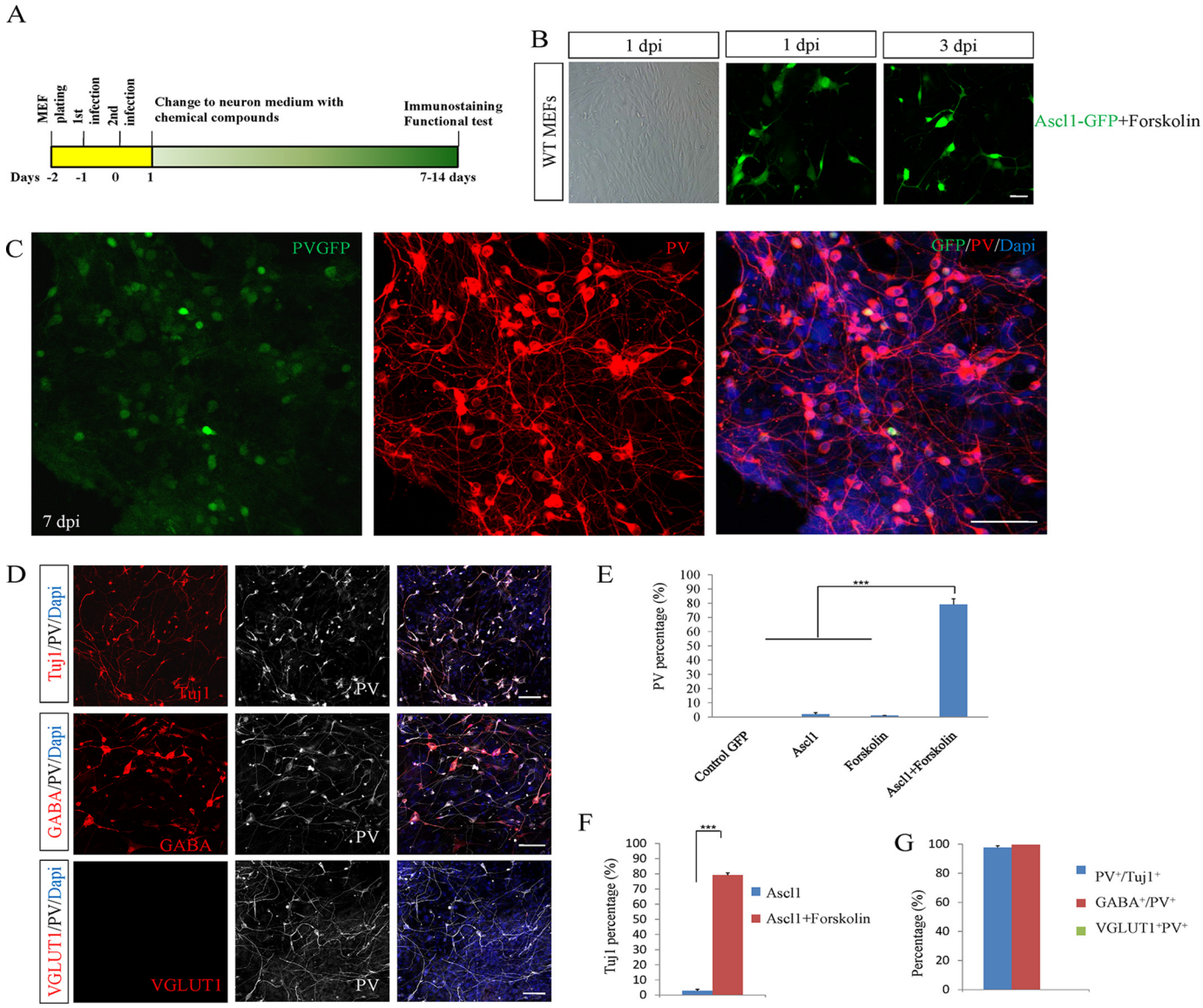

FIGURE 1. **Forskolin combined with Ascl1 efficiently converts fibroblasts into PV neurons.** *A*, diagram depicting the procedures for converting MEFs to neurons by adenoviruses carrying *Ascl1* combined with the chemical compound. *B*, WT MEFs isolated from wild-type mice were treated with Ascl1-GFP and forskolin; the cellular morphology started to change at 3 dpi. *C*, Ascl1 in coordination with forskolin effectively induced MEFs to PV-positive neurons as examined by PV at 7 dpi. *D*, almost all Ascl1- and forskolin-induced neurons were positive for GABA and negative for VGLUT1. PV, VGLUT1, and GABA staining were performed at 14 dpi. *E*, PV-positive cells were examined and counted at different conditions of GFP-control, Ascl1 alone, forskolin alone, and Ascl1 plus forskolin. *F*, Tuj1-positive cells were checked by the treatment of Ascl1 and Ascl1 plus forskolin. *G*, quantification of PV^+Tuj1^+, $GABA^+PV^+$, and $VGLUT1^+PV^+$ cells. ***$p < 0.001$; *NS* (not significant), $p > 0.05$. *Scale bars*: 50 μm.

Data were compared by *t* test, one-way analysis of variance (ANOVA) for multiple comparisons, or two-way ANOVA for repeated measures. Values were considered statistically significant at a difference at $p < 0.05$ (*), $p < 0.01$ (**), and $p < 0.001$ (***). Data are presented as the mean ± S.E.

Results

Identification of Forskolin as a Promising Candidate for iPV Neuron Generation—To reveal whether chemical compounds could induce fibroblast into PV neurons, we first set up a screen based on the established system for direct neuron generation. Because PV neurons are inhibitory neurons, we used the transcription factor Ascl1, which induces an inhibitory fate during neural specification, as the core factor. Compounds were added into culture medium after cells were infected Ascl1 first (Fig. 1*A*). Under this system we screened compounds at concentrations ranging from 1 μM to 100 μM. Part of the compounds screening results are provided at supplemental Table 1. Eventually, we identified one compound, named forskolin, that could efficiently induce PV-positive neurons at a concentration of 20 μM together with transcription factor Ascl1.

MEFs from wild-type and PV-GFP transgenic mice were used as the initial cells (14). MEFs were detected to be fibronectin- and fibroblast-specific protein 1 (FSP1, also called S100A4)-positive and Tuj1/GFAP/Nestin-negative. We did not observe Tuj1-positive cells in cultured MEFs after empty vector adenovirus infection or without viral infection. The cellular variation in morphology started at 3 days post infection (dpi) by the treatment of Ascl1-GFP virus and forskolin (Fig. 1*B*). The induced neurons became elaborately branched after another 2

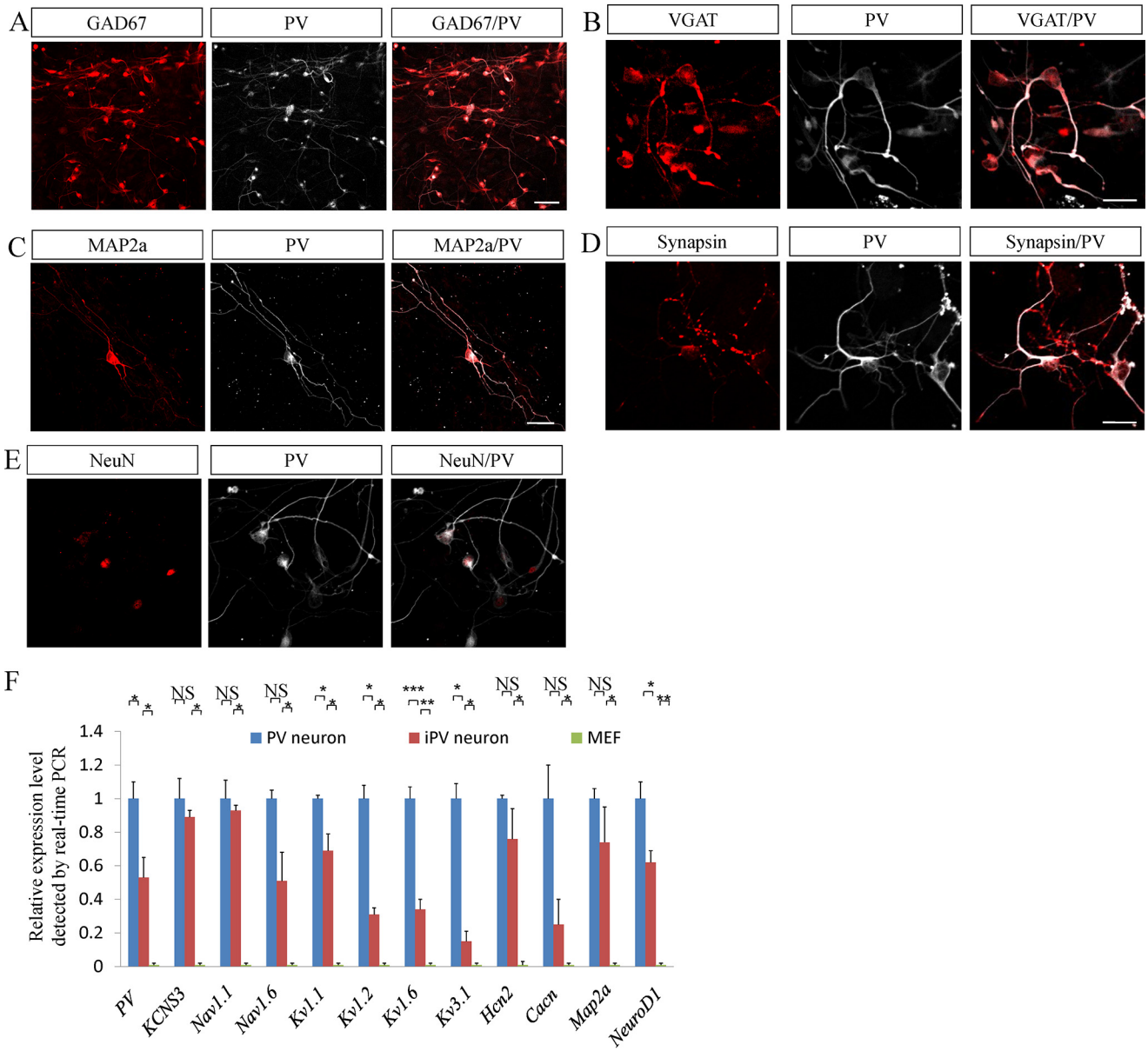

FIGURE 2. **iPV neurons express the specific markers of PV neurons.** *A* and *B*, at 14 days post-infections, MEF-derived iN cells expressed two specific inhibitory neuronal markers of GAD67 (*A*) and VGAT (*B*). *C–E*, at 10–14 days post-infection, iPV neurons expressed the pan-neuronal markers Map2a (*C*), synapsin (*D*), and NeuN (*E*) along with PV. *F*, real-time fluorescence quantification PCR showed that neuronal or PV-specific genes were up-regulated in iPV neurons, and this tendency is consistent with that in endogenous PV neurons. $*p < 0.05$, $**p < 0.01$, $***p < 0.001$. *NS* (not significant), $p > 0.05$. *Scale bars*: 50 μm.

days of culture, indicating the maturation of these converted neurons (Fig. 1*C*). At 7 dpi, PV-positive cells accounted for 77.2% of the total cells and were almost all Tuj1-positive neuronal cells (Fig. 1, *D–F*). However, Ascl1 alone and forskolin alone did not induce fibroblasts to PV neurons.

To further characterize the cellular identity of the induced PV cells, we stained the iPV neurons with antibodies against GABA and VGLUT1 at 14 dpi. In four replicates, we did not observe any VGLUT1-positive cells. Instead, nearly all PV-positive cells were GABA-positive (99.6% double positive; Fig. 1, *D* and *G*).

Forskolin drastically increased the induction of PV neurons in our screening system. We then asked whether forskolin alone was able to convert fibroblasts into PV neurons. In another set of MEFs that did not receive adenoviral infection of Ascl1, we administered the same amount of forskolin used in the above screen and examined the possible neuronal generation through immunostaining with Tuj1 and PV. During the 21 days of inspection, we did not find any Tuj1- or PV-positive cells in MEFs treated with forskolin alone, indicating that forskolin could act in combination with Ascl1to generate iPV neurons.

Characterization of iPV Neurons—First, we analyzed these iPV neurons with more specific-type neuronal markers. At 14 days post infection, MEF-derived iNs expressed two neuronal markers for inhibitory neurons, GAD67 and VGAT (Fig. 2, *A* and *B*). The iN cells were also positive for the neuronal markers Map2a, NeuN, and synapsin (Fig. 2, *C–E*).

The induction of PV neurons from MEFs was further verified by examining the gene expression in MEFs, iPV neurons, and endogenous PV neurons using real-time fluorescence quantitative PCR. Compared with that in MEFs, all of the neuron-spe-

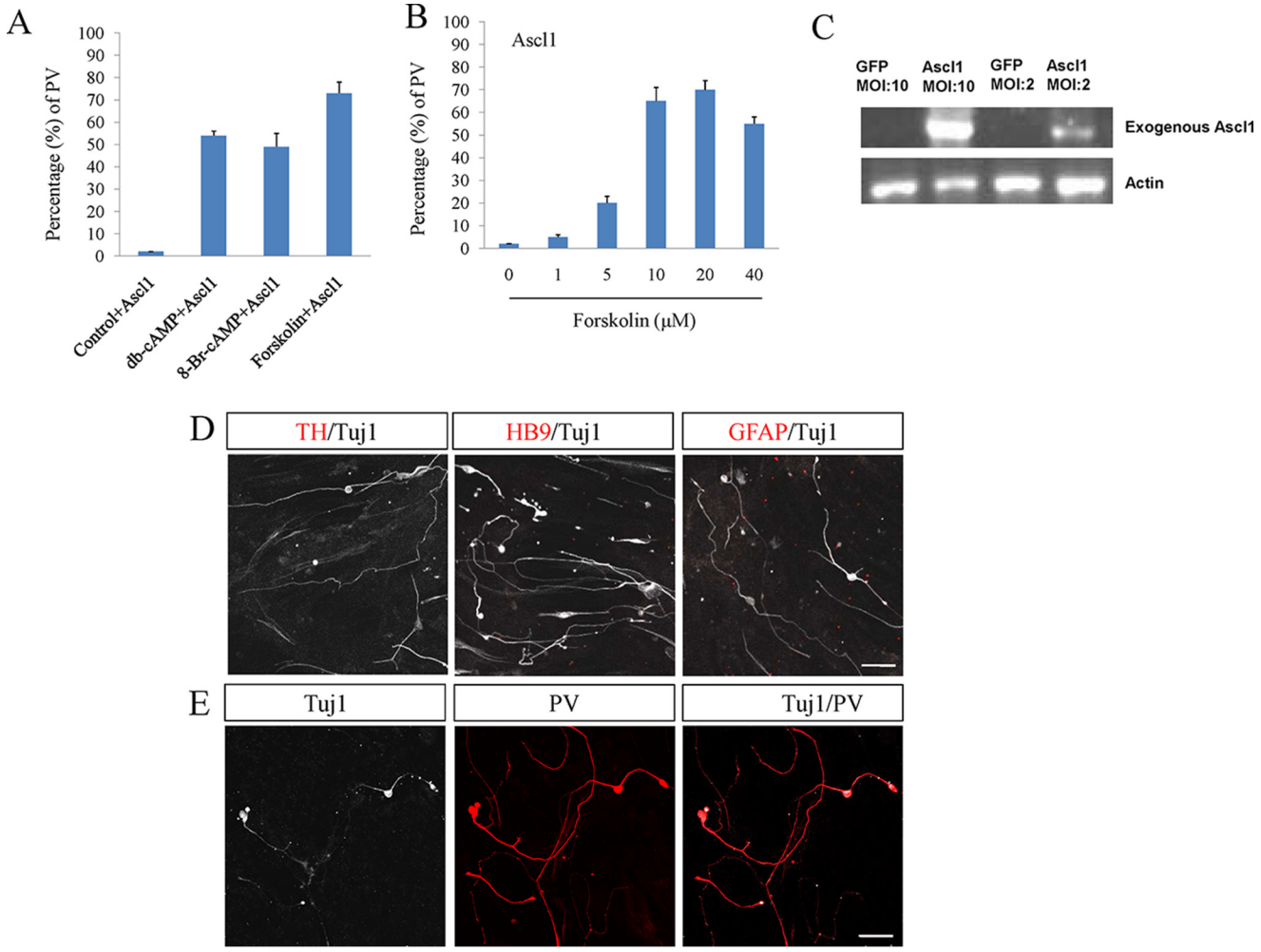

FIGURE 3. **Extensive examination of iPV neurons.** *A*, the effect of cAMP analog of Bt_2cAMP and 8-Br-cAMP on the conversion. *B*, dose-dependent manner of forskolin. *C*, exogenous Ascl1 expression was detected by RT-PCR. *D*, iPV neurons were checked by other specific neuronal markers of TH and HB9 and glial marker of GFAP. *E*, the conversion of adult tail-tip fibroblasts to neurons was examined by Tuj1 and PV staining. *Scale bars*: 50 μm.

cific genes were up-regulated in iPV neurons, which is comparable with that in endogenous PV neurons. The mature neuronal Map2a was dramatically increased >500-fold compared with MEF. The PV-neuron-specific genes encoding sodium voltage-gated channel and potassium voltage-gated channel members (15, 16) were up-regulated dozens or hundreds of times compared with MEF (Fig. 2*F*). This tendency for up-regulation was consistent with that in endogenous PV neurons.

Extensive Examination of PV Neuron Induction—Forskolin usually increases the level of cAMP. To determine whether cAMP analogs have a similar effect, Bt_2cAMP (dibutyryl cyclic AMP) and 8-Br-cAMP were applied to culture medium. These two cAMP analogs with Ascl1 could convert fibroblasts to neurons as well (Fig. 3*A*). The dose-dependent manner of forskolin was also checked, and forskolin had the high conversion effect at 10 or 20 μM (Fig. 3*B*). After infection with Ascl1, the expression of Ascl1 needed to be measured, and the result showed Ascl1 was highly expressed with multiplicity of infection (*MOI*) of 10 (Fig. 3*C*). iPV neurons were examined by more specific neuronal markers of TH and HB9 and glial marker of GFAP, which were not detected (Fig. 3*D*). To determine whether iPV neuron cells could also be obtained from postnatal cells, tail-tip fibroblasts from adult mice were used. The data showed Tail tip fibroblasts were also converted to iPV neurons (Fig. 3*E*).

Electrophysiological Detection of iPV Neuron—To determine the electrophysiological properties of Ascl1+forskolin iN neurons, we characterized the action potentials (AP) and PSCs of those iN cells at 7–14 days post infection. At 7 dpi, all iPV neurons ($n = 15$) have functional membrane properties including sodium and potassium currents (Fig. 4*A*). Sodium currents could be blocked by the specific inhibitor of TTX (Fig. 4*B*). iPV neurons exhibited repetitive action potentials with high frequency discharges and sharp spikes (Fig. 4*C*). The electrophysiological parameters of resting membrane potential, membrane input resistance, and membrane capacitance were measured in iPV neurons and endogenous PV neurons, which showed similarity (Fig. 4*D*). These characteristics are all features specific to PV neurons (17). At 7–10 dpi, spontaneous action potentials were detected and could be abolished by TTX (Fig. 4*E*). The spontaneous PSCs could not be abolished by CNQX+AP5, but they could be abolished by PTX, indicating that the PSCs in culture were inhibitory PSCs with inhibitory GABA neurotransmission (Fig. 4*F*). Finally, GABA could evoke PSCs in

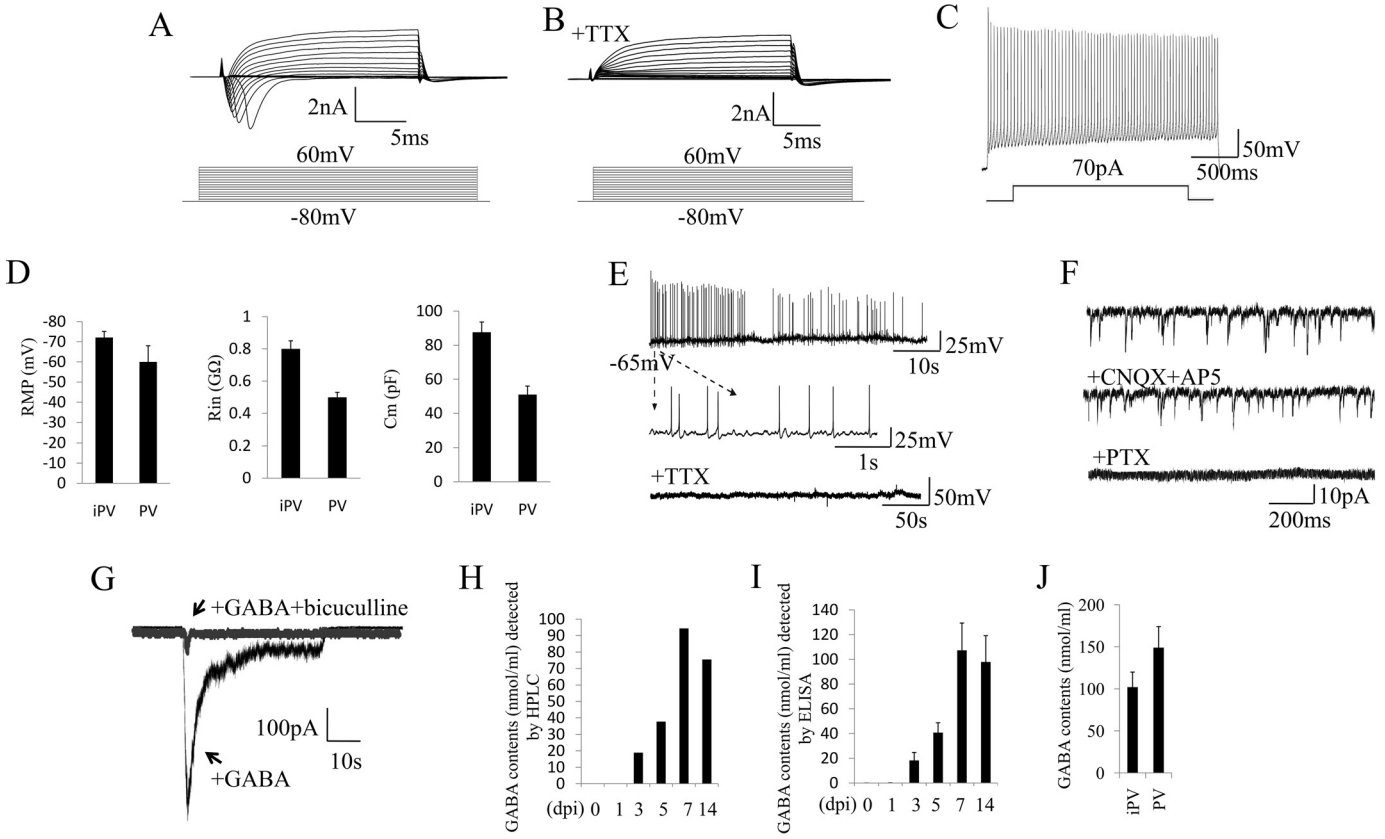

FIGURE 4. **Electrophysiological properties of iPV neurons.** *A*, representative traces of whole-cell currents in voltage-clamp mode at 7 days post infection. *B*, TTX could abolish the sodium currents. *C*, action potentials evoked by step-depolarization of the membrane in current-clamp mode at 7 days post infection. *D*, analysis of membrane properties including resting membrane potential (*RMP*), membrane input resistances (*Rin*), and membrane capacitance (*Cm*) in iPV neuron and endogenous PV neuron. *MΩ*, megaohms; *pF*, picofarads. *E*, iN cells show spontaneous action potentials, which could be inhibited by the application of TTX. *F*, iN cell spontaneous PSCs could not be reduced by CNQX+AP5 but could be abolished by PTX. *G*, GABA-evoked PSCs could be blocked by bicuculline. *H* and *I*, HPLC and ELISA detection demonstrate that GABA was released by induced PV neurons in the culture medium with a peak at 7 dpi. *J*, GABA level in iPV neuron and endogenous PV neuron.

the iPV neurons, and the evoked PSCs could be blocked by bicuculline (Fig. 4*G*).

To further explore the neurotransmitter-releasing properties of the iN cells, we collected the culture medium of iN cells from 1 to 10 days post infection. We then quantified the amount of GABA using either HPLC or ELISA. We found that the GABA concentration in the medium gradually increased over time and exceeded 100 ng/ml at 7 dpi. Thereafter, it remained at a similar level (Fig. 4, *H–J*). These *in vitro* data indicated that the iPV neurons were inhibitory neurons.

iPV Neurons Integrate into the Hippocampal Dentate Gyrus Neural Network—To verify whether the iPV neurons have functional properties *in vivo*, we transplanted these iPV neurons into the brains (18, 19). The iPV neurons were transplanted into the hippocampal dentate gyrus of mice. The grafted iPV neurons migrated alongside the hippocampal fissure during the following 4 weeks but did not exceed the boundary of the fissure (Fig. 5*A*). Two weeks after transplantation, iPV cells were examined for PV (Fig. 5*B*). After 4 weeks, NeuN- and synapsin-expressing iN cells were readily seen in the brain sections (Fig. 5, *C* and *D*). These data indicated that the transplanted iPV neurons could survive and become mature after transplantation into the brain.

After the grafted cells matured and grew for 8–10 weeks, we collected acute brain slices with a 300-μm thickness, put them in ice-cold artificial cerebrospinal solution, and characterized them using electrophysiological testing. The grafted cells that had been electrophysiologically recorded were also examined for PV staining (Fig. 4*E*). Furthermore, the GFP-positive cells had the ability to produce regular fast spiking pattern action potentials with high thresholds (Fig. 5*F*). The frequency of the grafted cell AP was 186 ± 22 Hz/s ($n = 3$), which was similar to the endogenous PV cell AP frequency of 160–210 Hz/s ($n = 5$). The grafted cell threshold of onset AP was >200 pA, and the maximum frequency threshold was ~600pA, which were also similar to the endogenous PV neuron AP threshold (Fig. 5*G*). More physiological parameters of the grafted cells were similar to the characteristics of endogenous PV neurons, such as resting membrane potential, capacitance, input resistance, electrical current, cell size, and input and output electrical signals. In addition, transplanted iPV neurons displayed miniature PSCs ($n = 7$), and the amplitude and frequency of those PSCs was similar to those of endogenous PV neurons ($n = 7$) (Fig. 5*H*).

Global Gene Expression Pattern Detection in iPV Neurons—To explore in more detail of the similarities and differences between iPV neurons and endogenous PV neurons, we compared the global gene expression pattern of MEFs, several stages of iPV neurons, and endogenous PV neurons using microarray analysis. Hierarchical clustering revealed that the global gene expression profile of iN cells showed a higher degree of similarity to primary

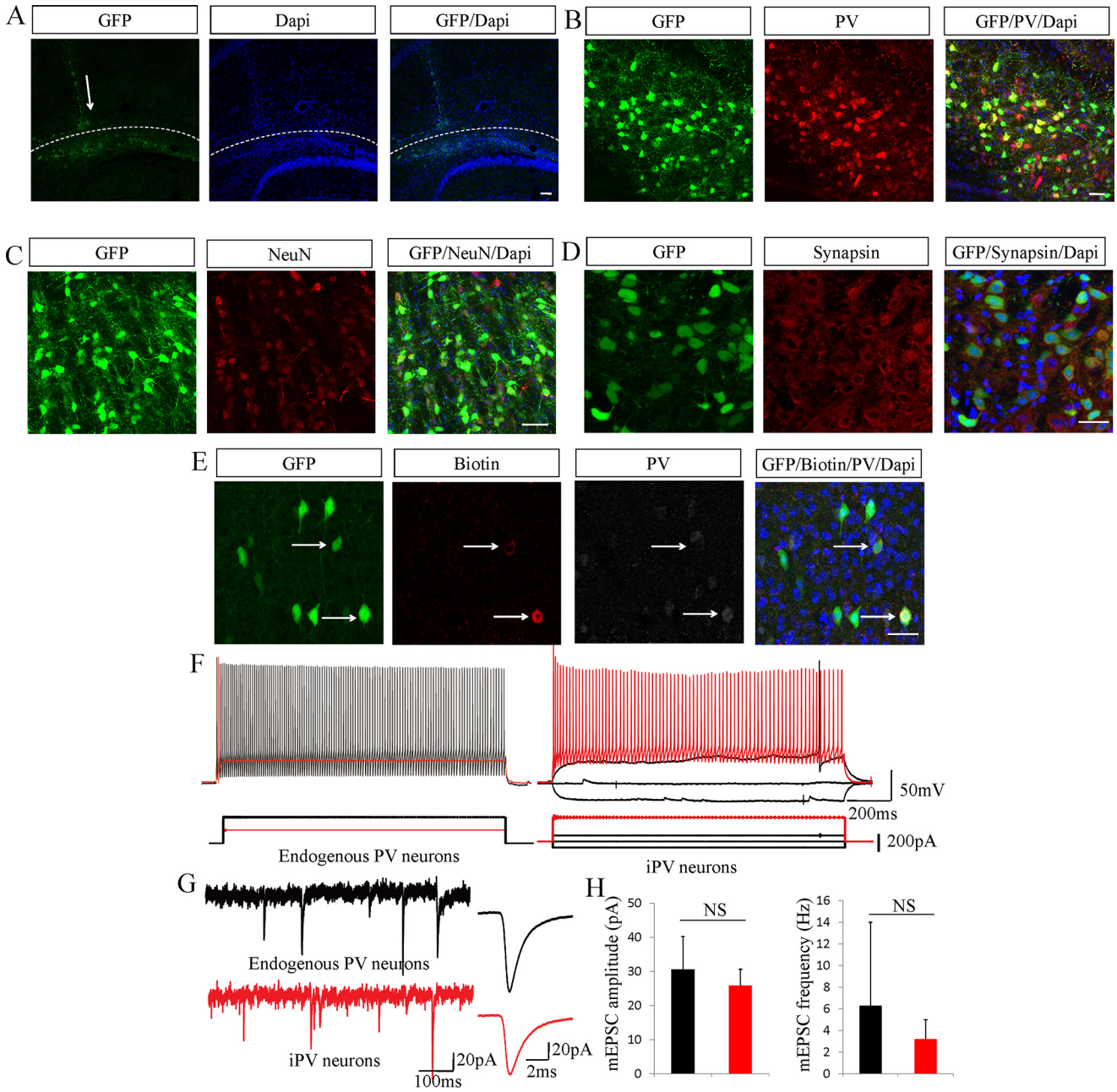

FIGURE 5. **iPV neurons integrate into hippocampal dentate gyrus neural networks *in vivo*.** *A*, a schematic diagram represents iN cell transplant position, and *arrows* denote grafted GFP+ cells in the hippocampal dentate gyrus after transplantation. *green*, GFP; *blue*, DAPI. *B–D*, 2–4 weeks after transplantation iN cells mature and express PV, NeuN, and synapsin. *E*, the grafted cells that had been electrophysiologically recorded were examined for the expression of PV. *F*, the action potentials showed high frequency discharges, sharp spikes, and high thresholds. *G*, the miniature PSCs were recorded in grafted cells *in vivo*. The *red bar* represents iPV neuron electrophysiological signals, and the *black bar* shows endogenous PV neurons. *H*, the amplitude and frequency of iPV neurons miniature PSCs were similar to endogenous PV neurons. The data are presented as the mean ± S.E. of the cell counts. *Scale bars*: 100 μm (*A*) and 50 μm (*B–E*). *NS*, not significant.

neurons rather than MEF cells. We found that 2175 genes with a >2-fold change were altered in iPV neurons compared with MEFs. The gene expression pattern between iPV neurons and endogenous PV neuron was similar (Fig. 6*A*).

In iPV neurons, functionally categorized genes associated with neurogenesis, synaptic transmission, and axonogenesis were up-regulated. The genes included Ngf, Gabra3, Calb2, Rarb, Gabrb2, Npy1r, snap25, and Sparcl1 (Fig. 5*B*). Functionally categorized genes associated with fibroblast activity and mitosis were down-regulated (Fig. 6*B*). For instance, S100A4, also known as FSP, was minimally expressed in iPV neurons and primary PV neurons, which indicated that iPV neurons had lost their initial MEF nature and gained neuron nature. We also highlighted the genes listed under the GO (Gene Ontology) biological process category "neurogenesis" during neural development and differentiation in the induced *PV*-GFP-positive neurons (Fig. 6*C*). The MEF-related genes, like mitosis, were repressed in induced PV neurons (Fig. 6*D*).

Discussion

Unlike other types of neurons that have already been comprehensively documented, the differentiation program that

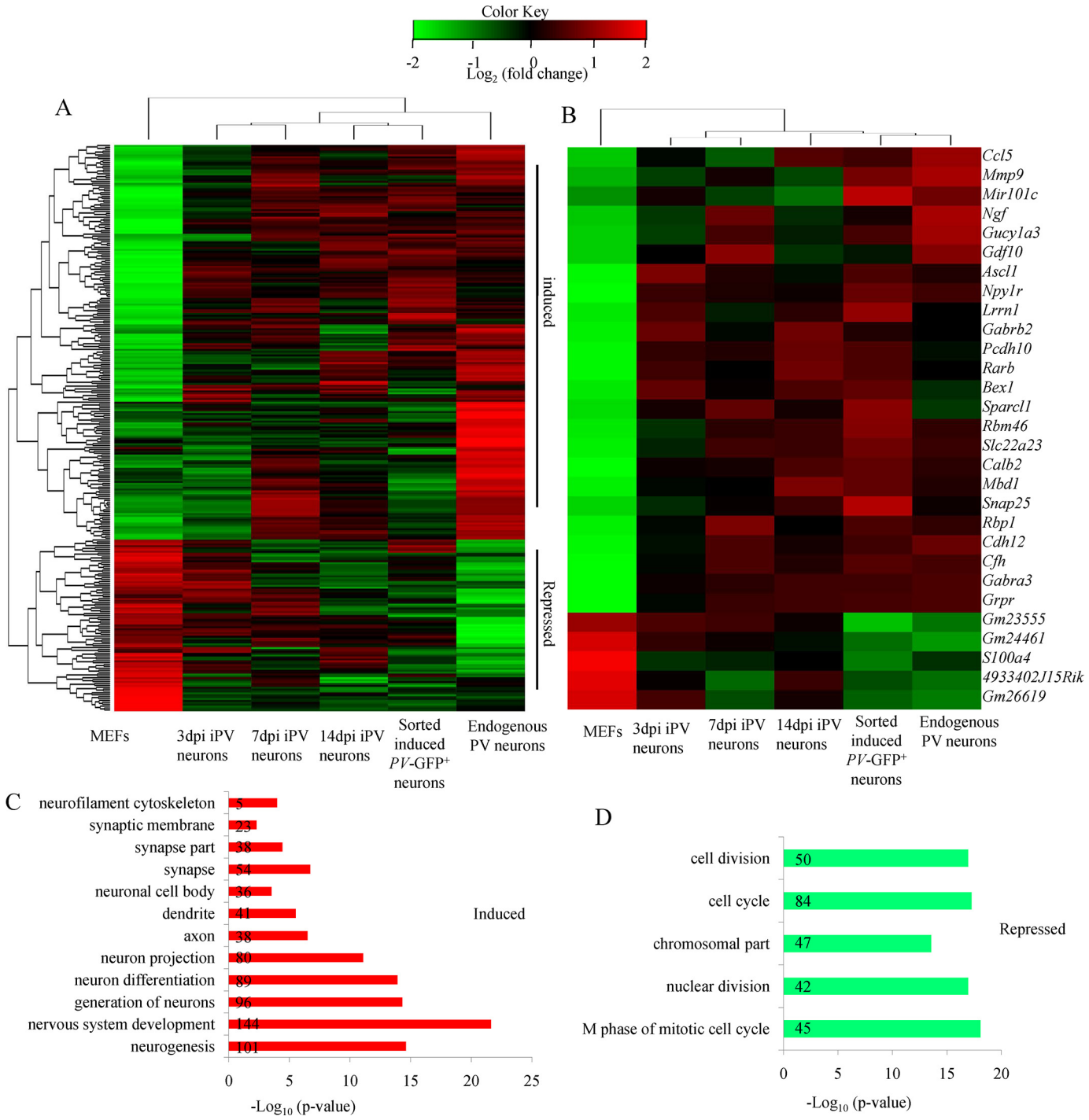

FIGURE 6. **Whole-genome gene expression profile of iPV neurons.** *A*, hierarchical clustering analysis of global gene expression patterns of MEFs, 3-dpi iPV cells, 7-dpi iN cells, 14-dpi iPV cells, sorted induced PV-GFP$^+$ cells from 14-dpi iPV cells, and endogenous PV neurons. Endogenous PV neurons were isolated from P20 *PV*-GFP mouse cortex. iPV cells were derived from MEFs at the corresponding days after Ascl1 + forskolin conversion. Approximately 300 differentiated genes among primary PV neurons and MEFs were selected for clustering analysis. Grouped induced and repressed genes are categorized as up-regulated or down-regulated genes compared with those in MEFs for both iPV cells and primary PV neurons. The gene expression profile in iPV cells is homoplastic to that in primary PV neurons. *B*, in iPV cells, functionally categorized genes associated with neurogenesis were up-regulated, and functionally categorized genes associated with fibroblast activity and mitosis were down-regulated. *C* and *D*, Gene Ontology (GO) analysis revealed the GO terms "neuron-" and "MEF-" related genes between induced *PV*-GFP-positive neurons and MEFs. The *numbers in the bar* represent how many genes participated in this process.

directs PV neuron specification and their essential roles in brain function and diseases are still under investigation (1, 2). The efficient generation of PV neurons for research and application has long been a challenge in the field. In this study we identified a chemical compound forskolin that, in combination with Ascl1, efficiently induced the generation of PV neurons from fibroblasts. The iPV neurons generated by this approach have function, as evidenced by the *in vitro* and *in vivo* characterization. This finding will be invaluable for the application of PV neurons to treat brain diseases and cure neuropsychiatric disorders.

Chemical compounds are a class of small molecules that are able to regulate the activity of proteins or signaling pathways in cells when added directly into culture. Over the last several years, abundant compounds have been identified that could increase the efficiency of induced pluripotent stem induction or replace certain transcription factors for reprogramming (20). Combinations of chemical compounds, with or without transcription factors, were able to accomplish the reprogramming of somatic cells (21, 22). Chemical compounds could also efficiently promote the generation of fibroblasts into neurons (13, 23, 24). In this background we screened chemical compounds and identified forskolin, a small molecule that could improve the generation of iPV neurons from fibroblasts. Although not effective alone, the administration of forskolin to fibroblasts that were adenovirally infected with Ascl1 dramatically converted the fibroblasts into iPV neurons with an incredible efficiency. Importantly, Ascl1 alone could not generate iPV neurons, although it was reported that Ascl1 could convert fibroblasts to neurons by co-culturing with glia cells (25). It is known that forskolin increases the cell level of cAMP. We found that cAMP analogs also promote the conversion in the presence of Ascl1. The data indicate that forskolin may act through the cAMP pathway during the conversion. Meanwhile, Ascl1 could activate the neuronal network. It is possible that the two important signaling pathways of activated cAMP signaling by forskolin and activated neuronal signaling by Ascl1 act together to push the fate of fibroblast to neuron. However, the detailed mechanism of the synergy between forskolin and Ascl1 in promoting iPV neuron induction still needs further investigation.

The great promises of transdifferentiation in regenerative medicine urge that converted cells, such as neurons, should be induced using safe approaches that neither prompt tumor formation nor result in other problems for the recipients. In this study, the iPV neurons were obtained from the adenoviral infection of a single transcription factor, Ascl1, supplemented with a chemical compound, forskolin. Adenoviruses rarely integrate into the host genome and, therefore, will minimally interfere with the gene expression profiles of the converted iPV neurons (11, 13). Chemical compounds, upon the removal from the culture system, will neither impact the function nor the behavior of the iPV neurons. Thus, the iPV neuron induction strategy we developed in this study minimizes the possible safety uncertainties and might be particularly promising for the generation of clinical-grade human iPV neurons for therapeutic purposes.

Author Contributions—Z. S. provided conception and design of the experiments, the main data collection, analysis, and manuscript writing. J. Z., S. C., Y. L., X. L., H. Q., and Q. Zhu provided partial data collection and analysis. B. H., Q. Zhou, and J. J. provided conception and design of the experiments and manuscript writing.

Acknowledgments—We are grateful to Zengqiang Yuan and Wanzhu Jin for critical comments and discussions, members of the Jiao laboratory for discussions, and Shiwen Li for technical assistance. We also thank Jianyuan Sun for electrophysiology work.

References

1. Hu, H., Gan, J., and Jonas, P. (2014) Interneurons. Fast-spiking, parvalbumin(+) GABAergic interneurons: from cellular design to microcircuit function. *Science* **345,** 1255263
2. Meyer-Lindenberg, A. (2010) From maps to mechanisms through neuroimaging of schizophrenia. *Nature* **468,** 194–202
3. Maroof, A. M., Keros, S., Tyson, J. A., Ying, S. W., Ganat, Y. M., Merkle, F. T., Liu, B., Goulburn, A., Stanley, E. G., Elefanty, A. G., Widmer, H. R., Eggan, K., Goldstein, P. A., Anderson, S. A., and Studer, L. (2013) Directed differentiation and functional maturation of cortical interneurons from human embryonic stem cells. *Cell Stem Cell* **12,** 559–572
4. Vierbuchen, T., Ostermeier, A., Pang, Z. P., Kokubu, Y., Südhof, T. C., and Wernig, M. (2010) Direct conversion of fibroblasts to functional neurons by defined factors. *Nature* **463,** 1035–1041
5. Pang, Z. P., Yang, N., Vierbuchen, T., Ostermeier, A., Fuentes, D. R., Yang, T. Q., Citri, A., Sebastiano, V., Marro, S., Südhof, T. C., and Wernig, M. (2011) Induction of human neuronal cells by defined transcription factors. *Nature* **476,** 220–223
6. Caiazzo, M., Dell'Anno, M. T., Dvoretskova, E., Lazarevic, D., Taverna, S., Leo, D., Sotnikova, T. D., Menegon, A., Roncaglia, P., Colciago, G., Russo, G., Carninci, P., Pezzoli, G., Gainetdinov, R. R., Gustincich, S., Dityatev, A., and Broccoli, V. (2011) Direct generation of functional dopaminergic neurons from mouse and human fibroblasts. *Nature* **476,** 224–227
7. Kim, J., Su, S. C., Wang, H., Cheng, A. W., Cassady, J. P., Lodato, M. A., Lengner, C. J., Chung, C. Y., Dawlaty, M. M., Tsai, L. H., and Jaenisch, R. (2011) Functional integration of dopaminergic neurons directly converted from mouse fibroblasts. *Cell Stem Cell* **9,** 413–419
8. Pfisterer, U., Kirkeby, A., Torper, O., Wood, J., Nelander, J., Dufour, A., Björklund, A., Lindvall, O., Jakobsson, J., and Parmar, M. (2011) Direct conversion of human fibroblasts to dopaminergic neurons. *Proc. Natl. Acad. Sci. U.S.A.* **108,** 10343–10348
9. Son, E. Y., Ichida, J. K., Wainger, B. J., Toma, J. S., Rafuse, V. F., Woolf, C. J., and Eggan, K. (2011) Conversion of mouse and human fibroblasts into functional spinal motor neurons. *Cell Stem Cell* **9,** 205–218
10. Liu, M. L., Zang, T., Zou, Y., Chang, J. C., Gibson, J. R., Huber, K. M., and Zhang, C. L. (2013) Small molecules enable neurogenin 2 to efficiently convert human fibroblasts into cholinergic neurons. *Nat. Commun.* **4,** 2183
11. Meng, F., Chen, S., Miao, Q., Zhou, K., Lao, Q., Zhang, X., Guo, W., and Jiao, J. (2012) Induction of fibroblasts to neurons through adenoviral gene delivery. *Cell Res.* **22,** 436–440
12. Lau, S., Rylander Ottosson, D., Jakobsson, J., and Parmar, M. (2014) Direct neural conversion from human fibroblasts using self-regulating and non-integrating viral vectors. *Cell Rep.* **9,** 1673–1680
13. Shi, Z., Shen, T., Liu, Y., Huang, Y., and Jiao, J. (2014) Retinoic acid receptor gamma (Rarg) and nuclear receptor subfamily 5, group A, member 2 (Nr5a2) promote conversion of fibroblasts to functional neurons. *J. Biol. Chem.* **289,** 6415–6428
14. Ango, F., Wu, C., Van der Want, J. J., Wu, P., Schachner, M., and Huang, Z. J. (2008) Bergmann glia and the recognition molecule CHL1 organize GABAergic axons and direct innervation of Purkinje cell dendrites. *PLoS Biol.* **6,** e103
15. Chow, A., Erisir, A., Farb, C., Nadal, M. S., Ozaita, A., Lau, D., Welker, E., and Rudy, B. (1999) K^+ channel expression distinguishes subpopulations of parvalbumin- and somatostatin-containing neocortical interneurons. *J. Neurosci.* **19,** 9332–9345
16. Georgiev, D., González-Burgos, G., Kikuchi, M., Minabe, Y., Lewis, D. A., and Hashimoto, T. (2012) Selective expression of KCNS3 potassium channel α-subunit in parvalbumin-containing GABA neurons in the human prefrontal cortex. *PloS ONE* **7,** e43904
17. Popowski, M., Templeton, T. D., Lee, B. K., Rhee, C., Li, H., Miner, C., Dekker, J. D., Orlanski, S., Bergman, Y., Iyer, V. R., Webb, C. F., and Tucker, H. (2014) Bright/Arid3A acts as a barrier to somatic cell reprogramming through direct regulation of Oct4, Sox2, and Nanog. *Stem Cell Reports* **2,** 26–35
18. Gröticke, I., Hoffmann, K., and Löscher, W. (2007) Behavioral alterations in the pilocarpine model of temporal lobe epilepsy in mice. *Exp. Neurol.*

207, 329–349
19. Hunt, R. F., Girskis, K. M., Rubenstein, J. L., Alvarez-Buylla, A., and Baraban, S. C. (2013) GABA progenitors grafted into the adult epileptic brain control seizures and abnormal behavior. *Nat. Neurosci.* **16,** 692–697
20. Zhu, S., Wei, W., and Ding, S. (2011) Chemical strategies for stem cell biology and regenerative medicine. *Annu. Rev. Biomed. Eng.* **13,** 73–90
21. Hou, P., Li, Y., Zhang, X., Liu, C., Guan, J., Li, H., Zhao, T., Ye, J., Yang, W., Liu, K., Ge, J., Xu, J., Zhang, Q., Zhao, Y., and Deng, H. (2013) Pluripotent stem cells induced from mouse somatic cells by small-molecule compounds. *Science* **341,** 651–654
22. Li, Y., Zhang, Q., Yin, X., Yang, W., Du, Y., Hou, P., Ge, J., Liu, C., Zhang, W., Zhang, X., Wu, Y., Li, H., Liu, K., Wu, C., Song, Z., Zhao, Y., Shi, Y., and Deng, H. (2011) Generation of iPSCs from mouse fibroblasts with a single gene, Oct4, and small molecules. *Cell Res.* **21,** 196–204
23. Hu, W., Qiu, B., Guan, W., Wang, Q., Wang, M., Li, W., Gao, L., Shen, L., Huang, Y., Xie, G., Zhao, H., Jin, Y., Tang, B., Yu, Y., Zhao, J., and Pei, G. (2015) Direct conversion of normal and Alzheimer's disease human fibroblasts into neuronal cells by small molecules. *Cell Stem Cell* **17,** 204–212
24. Li, X., Zuo, X., Jing, J., Ma, Y., Wang, J., Liu, D., Zhu, J., Du, X., Xiong, L., Du, Y., Xu, J., Xiao, X., Wang, J., Chai, Z., Zhao, Y., and Deng, H. (2015) Small molecule-driven direct reprogramming of mouse fibroblasts into functional neurons. *Cell Stem Cell* **17,** 195–203
25. Chanda, S., Ang, C. E., Davila, J., Pak, C., Mall, M., Lee, Q. Y., Ahlenius, H., Jung, S. W., Südhof, T. C., and Wernig, M. (2014) Generation of induced neuronal cells by the single reprogramming factor ASCL1. *Stem Cell Reports* **3,** 282–296